Effect of clay modification on structureproperty relationships and thermal degradation kinetics of β-polypropylene/clay composite materials

Reference:

Papageorgiou Dimitrios G., Filippousi Maria, Pavlidou Eleni, Chrissafis Konstantinos, van Tendeloo Gustaaf, Bikiaris Dimitrios.- Effect of clay modification on structureproperty relationships and thermal degradation kinetics of β-polypropylene/clay composite materials

Journal of thermal analysis and calorimetry - ISSN 1388-6150 - 122:1(2015), p. 393-406

DOI: http://dx.doi.org/doi:10.1007/s10973-015-4705-y

Effect of clay modification on structure-property relationships and thermal degradation kinetics of β-polypropylene/clay composite materials

Dimitrios G. Papageorgiou[1], Maria Filippousi[2], Eleni Pavlidou[1], Konstantinos Chrissafis[1*], Gustaaf Van Tendeloo[2], Dimitrios Bikiaris[3*]*

[1]Solid State Physics Section, Physics Department, Aristotle University of Thessaloniki, 541 24 Thessaloniki, Greece
[2]EMAT, University of Antwerp, Groenenborgerlaan 171, B-2020 Antwerp, Belgium
[3]Laboratory of Polymer Chemistry and Technology, Department of Chemistry, Aristotle University of Thessaloniki, GR-541 24, Thessaloniki, Greece

Abstract

The influence of neat and organically-modified montmorillonite on the structure-property relationships of a β-nucleated polypropylene matrix has been thoroughly investigated. High angle annular dark field scanning transmission electron microscopy revealed that the organic modification of clay facilitated the dispersion of the clay, while X-ray diffractograms showed the α-nucleating effect of the clays on the β-nucleated matrix. The results from tensile tests showed that the organic modification of MMT affected profoundly only the tensile strength at yield and at break. The effect of the organic modification of the clay on the thermal stability of the composites, was finally evaluated by thermogravimetric analysis, where the samples filled with oMMT decomposed faster than the ones filled with neat MMT, due to the decomposition of the organic salts which were initially used for the modification of MMT. A kinetics study of the thermal degradation of the composites was also performed, in order to export additional conclusions on the activation energy of the samples.

Keywords: composites, montmorillonite, β-polypropylene, mechanical properties, thermal degradation, HAADF-STEM

Corresponding Authors: Dimitrios Bikiaris (dbic@chem.auth.gr), Dimitrios G. Papageorgiou (dpapage@auth.gr), Konstantinos Chrissafis (hrisafis@physics.auth.gr)

1. Introduction

The development of the very interesting and high-performing group of materials named polymer nanocomposites initiated from the pioneering works of the Toyota group who incorporated clays in nylon 6 [1] and studied in detail the mechanical properties [2] of the first polymer/clay hybrid material. Over the past twenty years the specific category of polymer nanocomposites has been studied in detail and a vast number of polymer/clay composites have been developed [3-6]. The enhancement of the properties of the polymeric matrix due to the addition of a small amount of clay, has been attributed to several factors, such as the particle volume fraction, the particle volume ratio, the dispersion and orientation of the clay sheets, strength of interactions and others [7-14]. Also various modifications of the clays have been attempted in order to increase the interatomic distance between the clay sheets and facilitate in this way the exfoliation of the sheets of clay, lower the surface energy of the silicate surface and improve the wetting of the surface, facts which usually attribute better physical properties to the composite sample [15-20].

Apart from the significant presence of the inorganic filler, the physicochemical properties of the multicomponent polymer composite system are essentially dependent on the polymeric matrix that has been used. Polypropylene is one of the most popular semicrystalline polymers, existing in various crystalline forms, such as the monoclinic α-form and the trigonal β-form. Each crystalline phase attributes different characteristics to the matrix [21-25] and the insertion of each crystalline form is one of the most straightforward ways to alter the properties of the polymer. β-nucleating agents have been extensively used in order to improve the elongation at break and the impact toughness of polypropylene, which is very low compared with other polymers like polyethylene, in expense of other properties such as the modulus of elasticity or the tensile strength at yield [26-28]. For this reason inorganic fillers (such as MWCNTs and clays) are commonly used in order to enhance the deteriorating tensile properties of a β-nucleated polypropylene matrix [29-36].

In the present work, natural (Cloisite Na+) and modified montmorillonite with dimethyl dihydrogenated tallow quaternary ammonium (Cloisite 15A) were incorporated at different loadings, ranging from 0.5 to 5 wt.%, simultaneously with a β-nucleated agent into propylene/ethylene random copolymer. Even though Cloisite 15A presents a higher intergallery

spacing than neat montmorillonite and this could have a more pronounced effect on mechanical properties, it presents a major drawback. It decomposes at significantly lower temperatures (close to 200^{o}C) [37] and this can be a problem not only for the thermal stability of the composite samples but also for the preparation procedure of the samples. For this reason, in our case the polymeric matrix was co-polymerized with ethylene at a small amount (7%), which lowered the melting point of the matrix and therefore, the organically modified montmorillonite was not affected by the temperatures selected during the melt-mixing process.

The present work aims to investigate in detail the physicochemical properties of the propylene/ethylene random copolymer matrix in which neat and organically modified montmorillonite were inserted simultaneously with a β-nucleated agent. Additionally, the main objective was to observe the synergistic or competitive effect of each additive on the mechanical and thermal properties of the used polymer matrix.

2. Experimental

2.1 Materials and Methods

Polypropylene random copolymer (PP-R) was supplied by Basell Polyolefines with the commercial name Hostalen PP H5416 Random Copolymer containing 7 wt.% ethylene content and melt flow rate 0.29 g 10 min^-1 (190^{o}C/5 kg). The examined clay types were purchased from Southern Clay Products (Gonzales, TX). Cloisite Na+ is the pure, non-modified form of the montmorillonite clay (MMT-Na+). Closite 15A is modified with di (dehydrogenated tallow dimethyl ammonium) ions [2 HTM_2], where HT had the approximate composition 65% C18, 30% C16, and 5% C14. The specific density of Cloisite 15A was 1.66 g cm^-3 [38]. The calcium pimelate nucleator was synthesized by double decomposition as described in a previous study [39].

2.2 composites preparation

PPR/MMT and PPR/oMMT composites containing 0.5, 1, 2.5, 3.5 and 5 wt.% of neat and organically modified montmorillonite were prepared by melt-mixing in a Haake–Buchler Rheomixer (model 600) at 200^{o}C and 30 rpm for 15 min. During the preparation of the composites the β-nucleating agent (calcium pimelate) was added at a concentration of 1 wt.%.

Prior to melt-mixing, the particles were dried by heating in a vacuum oven at 100^{o}C for 24 h. The components were physically premixed before being fed into the rheomixer. In order to achieve a better dispersion of the montmorillonite in PPR, a RETSCH planetary ball mill model S100 was used. The PPR flakes along with the proper amount of MMT were fed into a 'C' type stainless steel grinding jar with a capacity of 25 ml. Five steel spheres were also added as a grinding medium. The milling was set at 500 rpm for a period of 1 hour. The physicochemical properties of the materials prior and after the milling process were tested, and no significant differences were observed. The preparation of all samples for the characterization procedure involved hot pressing of the extrudates in order to take the form of films of various thicknesses and sizes (depending on the characterization technique) and afterwards quenching into cold water. According to this way, any possible differences between the samples due to the processing conditions, were eliminated.

2.3 High Angle Annular Dark Field Scanning Transmission Electron Microscopy (HAADF-STEM)

Samples suitable for HAADF-STEM measurements were sectioned using a Leica UC7 ultramicrotome equipped with a FC7 cryo chamber and the sections had a thickness of 100–120 nm. The sections were placed on Quantifoil C coated Cu grids. Samples were cut at -80°C. HAADF-STEM images were acquired using a FEI Tecnai G2 electron microscope operated at 200 kV.

2.4 X-Ray Diffraction (XRD)

XRD analysis was performed on the polymeric matrix and the composites using a Rigaku Ultima+ diffractometer using Cu Kα radiation, a step size of 0.05° and a step time of 3 s, operating at 40 kV and 30 mA.

2.5 Mechanical Properties

Measurements of tensile mechanical properties of the prepared composites were performed on an Instron 3344 dynamometer, in accordance with ASTM D638, using a crosshead speed of 50 mm/min. Thin films of about 350 ± 25 μm were prepared using an Otto Weber, Type PW 30

hydraulic press, at a temperature of 195±5^{o}C. The moulds were rapidly cooled by immersing them in water at 20^{o}C. From these films, dumb-bell-shaped tensile test specimens (central portions 5 × 0.5 mm thick, 22 mm gauge length) were cut in a Wallace cutting press and conditioned at 25^{o}C and 55–60% relative humidity for 48 h. From stress-strain curves, the values of tensile strength at yield point and at break, elongation at break and Young's modulus were determined. At least five specimens were tested for each sample and the average values, together with the standard deviations, are reported.

Izod impact tests were performed using a Tinius Olsen apparatus in accordance with ASTM D256 method. The size of the specimen for the impact testing was 65 x 13 x 3 mm while their thickness was 4-5 mm. Five measurements were conducted for each sample, and the results were averaged to obtain a mean value.

2.6 Thermogravimetric Analysis (TG)

Thermogravimetric analysis was carried out with a SETARAM SETSYS TG-DTA 16/18. Samples (5.0 ± 0.2 mg) were placed in alumina crucibles. An empty alumina crucible was used as reference. All materials were heated from ambient temperature to 550 °C in a 50 ml min^-1 flow of nitrogen at a heating rate of 20°C min^-1. Continuous recordings of sample temperature, weight and heat flow were performed. In order to proceed to the thermal degradation kinetics study, the experiments were performed at 3 additional heating rates, namely 5, 10, 15 and 20^{o}C min^-1 according to the recommendations of ICTAC [40, 41].

3. Results and discussion

3.1 High Angle Annular Dark Field Scanning Transmission Electron Microscopy (HAADF-STEM)

One of the most important parameters which affect the general behavior of polymer (nano)composites, is the dispersion of the filler in the polymeric matrix. Therefore HAADF-STEM measurements were carried out with the aim of gaining insights on the relationship between microscopic structure and mechanical properties. The HAADF-STEM images (Figures

1 and 2) provide information concerning the morphology and the distribution of both MMT and organically-modified MMT inside the polymeric matrix.

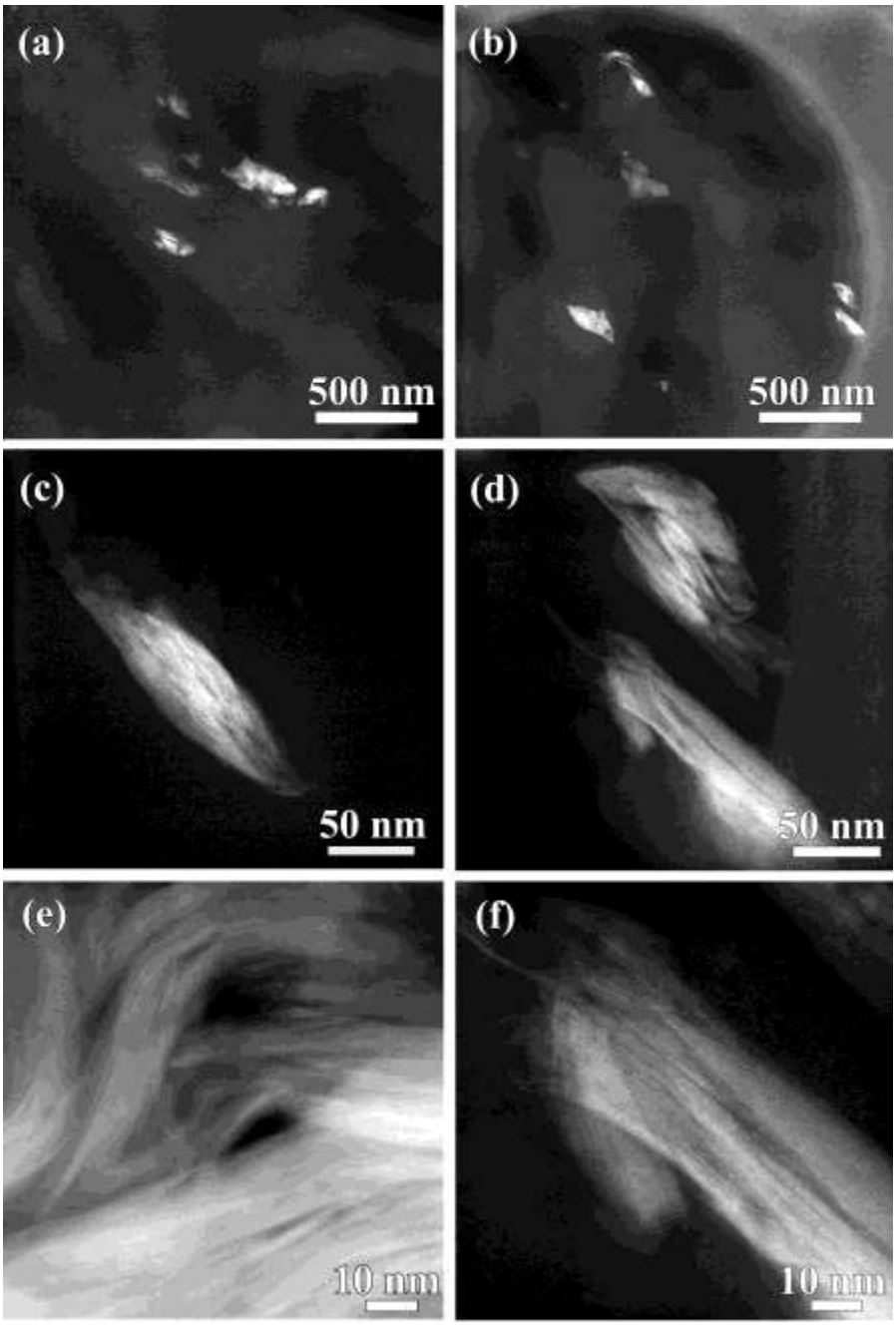

Figure 1. Low and high magnification HAADF-STEM images of the PPR-MMT sample with concentration 2.5 wt.% (a,c and e) and 1wt.% (b, d and f), showing the dispersion of the expanded montmorillonite particles (brighter features) inside the polymeric matrix. It can be seen

that the small distance between the clay layers obstructs the infiltration of the polymeric matrix, which eventually leads to the formation of aggregates.

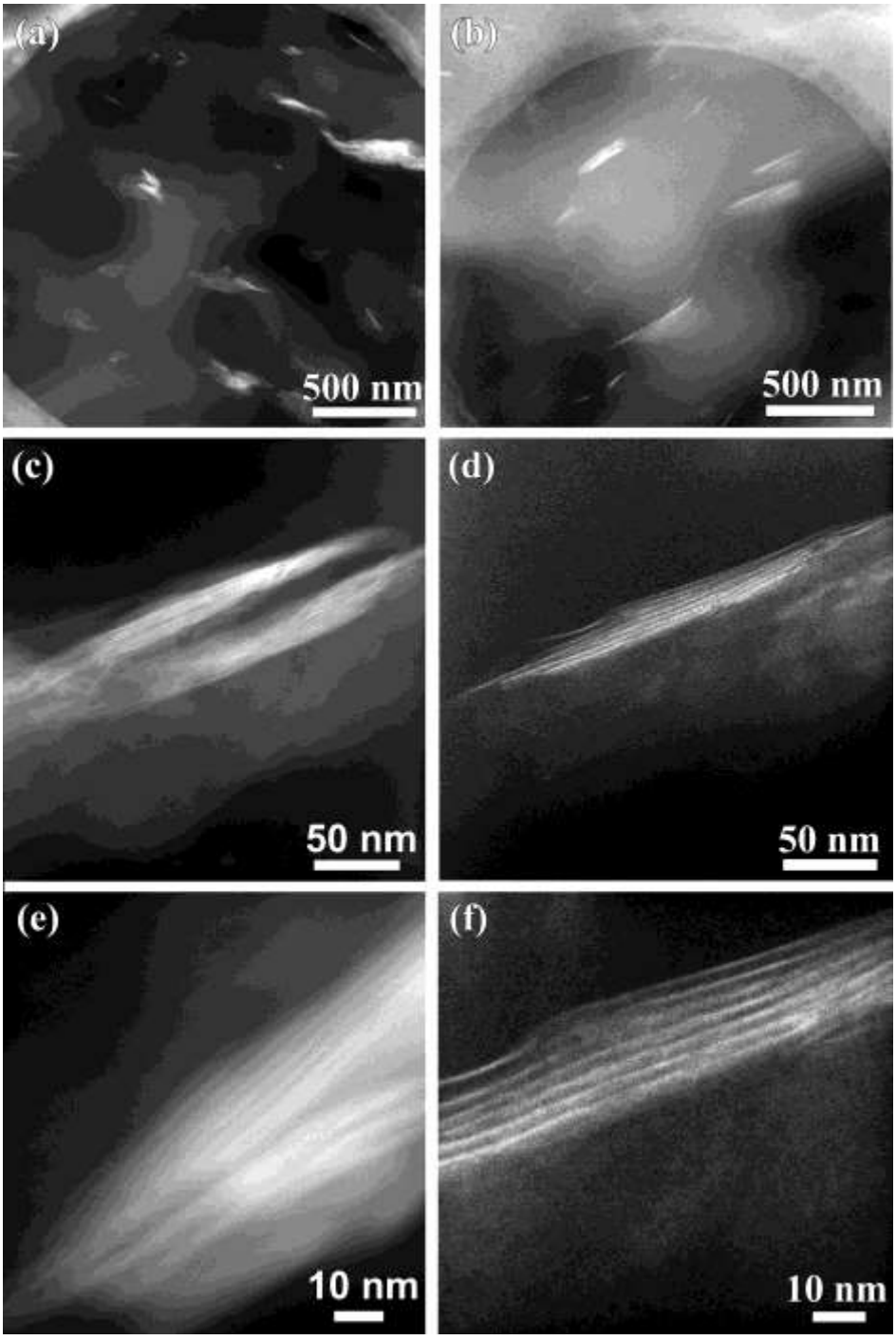

Figure 2. Low and high magnification HAADF-STEM images of the PPR-oMMT sample with concentration 2.5 wt.% (a, c and e) and 1 wt.% (b, d and f). The layers of the oMMT are distinct in images (c, d, e and f). From this image the intercalation phenomena between the polymeric matrix and the clay can be observed, since the stacks of clay are not independently dispersed inside the matrix.

In both sets of composites the clays are quite efficiently dispersed inside the polymer matrix and only at higher clay content, some aggregates are formed. However, it is clear that there are some differences between the arrangement of the stacks at the MMT and the oMMT. The main difference arises from the fact that an organic modification was applied on the neat montmorillonite with the use of quaternary ammonium salts. For this reason the aggregates are smaller and they are present to a lower extent in the composites containing oMMT. Furthermore, the distance between the clay stacks increased due to this modification, thus the polymer macromolecules are able to infiltrate easier between the clay stacks for the PPR/oMMT samples, as it can be observed from the illustrative HAADF-STEM images for two different concentrations (2.5 wt.% and 1 wt.%). This is even more obvious in Figures 2e, f. However, the modification of the clay by itself was not sufficient to prepare completely exfoliated clay structures inside the PPR matrix.

3.2 X-Ray Diffraction

Wide angle X-ray diffraction experiments were performed on quenched composite samples and the results can be seen in Figure 3. From these diffractograms it is clear that neat PPR forms β-crystals due to the addition of calcium pimelate, since a small peak is recorded at 16.1^{o}, which is characteristic of the β-crystals. However, this peak disappears in the case of the composite samples. Various literature reports have indicated the strong α-nucleating ability of montmorillonite [42-44], thus the quenching procedure [45] and the presence of clay resulted in composites solely presenting the α-crystalline structure. The specific phenomenon has been thoroughly investigated by Zheng et al. [46]. The effect of the presence of both types of clays on the crystallinity percentage was evaluated from the well-known equation:

$$X_c = \frac{A_c}{A_c + A_a} \quad (1)$$

where A_c and A_α are the areas under the crystalline peaks and amorphous halo respectively. A deconvolution of the X-ray diffractograms was performed prior to the calculations in order to estimate the area under each peak. The results are presented in Table 1 and it can be seen that the presence of the fillers inside the polymeric matrix triggers a drop in the crystallinity percentage. This is most probably caused by the decreased mobility of the macromolecular chains, due to the confinement effect from the clays, and has as result the lowering of the X_c [47, 48].

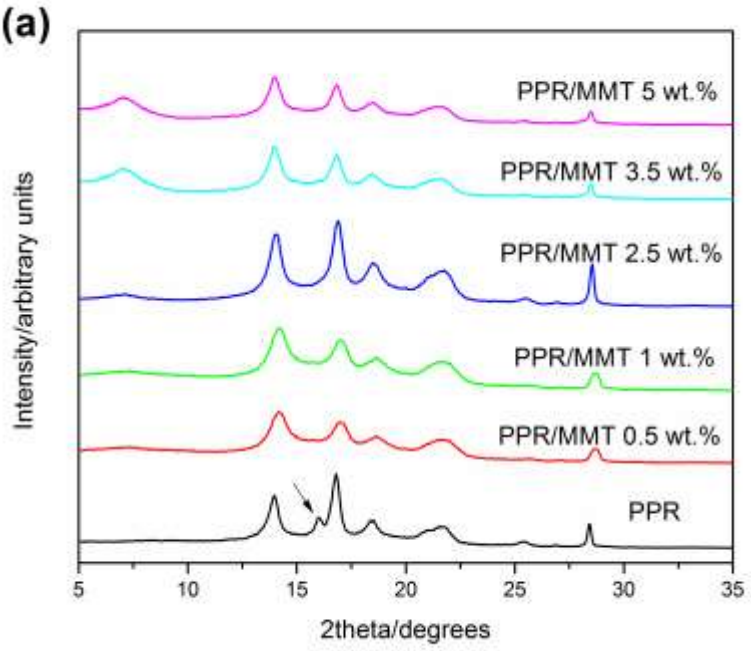

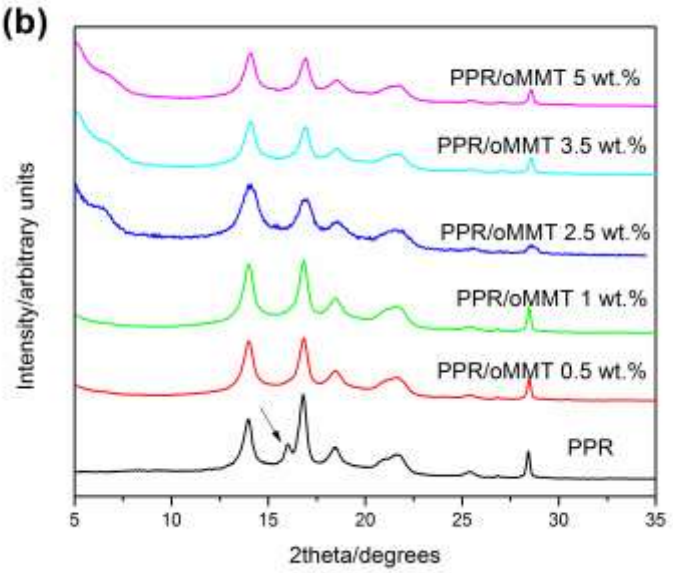

Figure 3. X-ray diffractograms of quenched composite samples.

Table 1. Calculated values of crystallinity for the composite samples.

a/a	MMT content/ wt.%	X_c/%	oMMT content/ wt. %	X_c/%
1	0	53.9	0	53.9
2	0.5	41.9	0.5	41.5
3	1	43.5	1	42.2
4	2.5	45.2	2.5	41.7
5	3.5	43.3	3.5	42.4
6	5	43.6	5	42.7

3.3 Mechanical Properties

The mechanical behavior of the composites was examined during tensile testing. The values of the modulus of elasticity, yield strength, stress and elongation at break were calculated from the stress-strain curves for each sample. In some previous works from our group, the way that the crystalline structure of polypropylene affects each time the final mechanical properties of the

polymeric matrix, has been discussed [28, 49, 50]. From the X-ray diffraction study, it was shown that the quenched composites crystallize in the α-form of polypropylene, therefore the significantly lower deformability of the α-lamellae is expected to play a significant role in the final mechanical properties. The results from the tensile testing of the composites are presented in Figure 4.

The elastic modulus of the composites does not present significant differences due to the different filler types, while it increases almost linearly for both sets of composites, indicating the strong reinforcing effect of each clay type and the effective stress transfer mechanism from the polymeric matrix, to the clay sheets. Regarding the tensile strength at yield, it can once again be seen that the clay type does not affect the yield values significantly, since the differences between the two sets of samples are small. For both sets, a significant initial increase of yield can be observed for the samples filled with 0.5 and 1 wt.% of clay, demonstrating that the better dispersion of the clays inside the polymeric matrix at low filler contents, as confirmed by HAADF-STEM measurements, enhances the interfacial interactions between the polymer and the filler. From that point and on, the yield values remain almost stable, due to the low intercalation phenomena and only in oMMT some higher values are recorded at clay contents above 2.5 wt%. This is due to the better dispersion of oMMT compared with neat MMT. A similar behavior can be seen in tensile strength at break; it presents an increase for low filler contents, due to better dispersion or partial exfoliation of clays, while from that point and on, it presents a quite stable behavior in oMMT composites or a small decrease in MMT composites. In addition, the composites exhibit a significantly lower elongation than the polymeric matrix due to the confinement effect induced in the macromolecular chains of the neat polymer by the filler. Furthermore, the increasing number of aggregates with increasing filler content plays a very significant role in the elongation properties due to the fact that the aggregates act as stress concentrators and possible failure points during tensile testing.

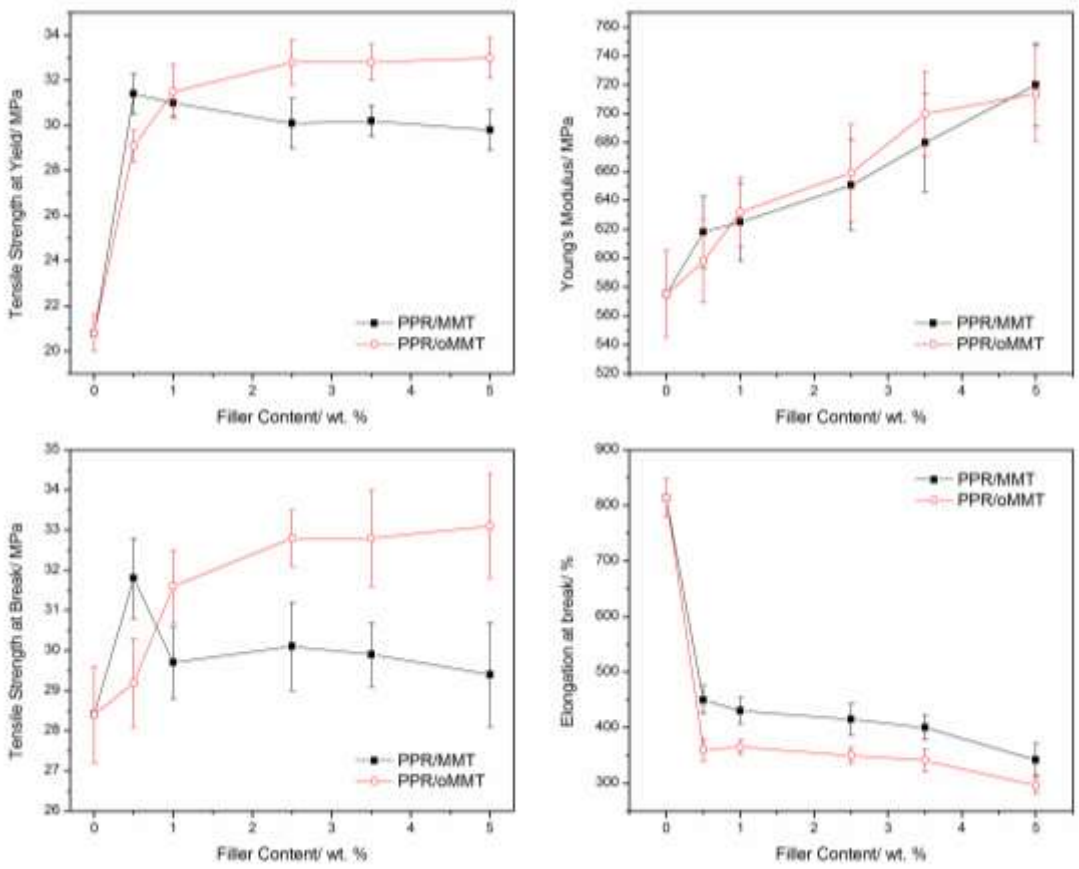

Figure 4. Mechanical properties of PPR/MMT and PPR/oMMT composites

3.3.1 Impact Testing

The behavior of the composite materials during impact is presented in Figure 5. It can be seen that the presence of both clay types lowers the impact resistance of every sample. It has been proved that α-nucleated polypropylene presents lower resistance than β-nucleated one, since β-polypropylene presents extended plastic (damage) zone due to the higher deformability of the β-spherulites [51]. On the contrary, α-polypropylene presents a typical brittle fracture. Thus, the composites were expected to present a lower impact resistance since they were crystallized mainly in the α-form. At higher filler contents, the formation of aggregates also plays a role in the final impact properties. From these results it can be also said that the inhibition of β-crystal formation from the addition of both types of clays may have a negative effect on impact strength of composites.

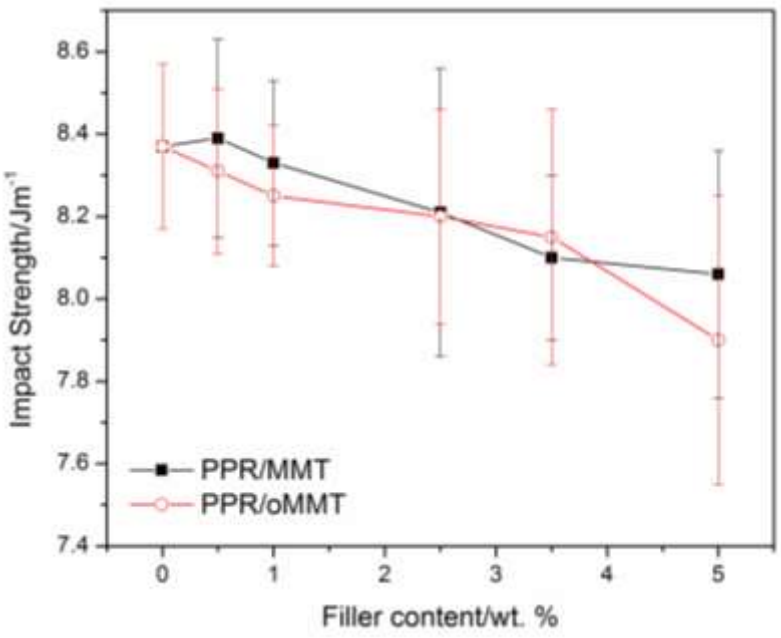

Figure 5. Impact strength of PPR/MMT and PPR/oMMT composites

3.3.2 Modeling of the modulus of elasticity

The prediction of the mechanical behavior of composite materials has been a difficult subject for many scientists over the last decades. The fact that many and different factors such as the polymeric matrix, the size, the geometry and the direction of the filler, the quality of adhesion, the densities of the components and others affect in a different way the behavior of the material, make this task very challenging. Also, the fact that the majority of those theories was developed for micro-composite and not -composite systems, makes the successful application of them even more difficult. Initially, the simple theory proposed by Guth [52], which can be applied for rod-like filler particles embedded in a polymeric matrix, is expressed by the following equation:

$$\frac{E_c}{E_m} = 1 + 0.67 f V_f + 1.62 f^2 V_f^2 \quad (2)$$

where E_c and E_m are the modulus of the composite and the matrix respectively, V_f is the volume fraction of the filler and f is a shape factor (i.e. length/width) [53].

Wu modified the popular approach by Guth, by introducing a modulus reduction factor (MRF) [54]. Its value was estimated to be 0.66 and it was multiplied by the shape factor *f*:

$$\frac{E_c}{E_m} = 1 + 0.67(MRF) f V_f + 1.62(MRF) f^2 V_f^2 \tag{3}$$

Ishai and Cohen [55] and Paul [56] assumed that the two components of the composite system are in a state of homogeneous stress and that the adhesion is perfect at the interface of a cubic inclusion in a cubic matrix. Thus the equation proposed by Paul is:

$$\frac{E_c}{E_m} = 1 + \frac{1 + (\delta - 1) V_f^{2/3}}{1 + (\delta - 1)(V_f^{2/3} - V_f)} \tag{4}$$

which is an upper-bound solution, according to the well-known Voigt-Reuss bounds [57] and where $\delta = E_f / E_m$. Ishai and Cohen proposed a lower-bound solution:

$$\frac{E_c}{E_m} = 1 + \frac{V_f}{\frac{\delta}{(\delta - 1)} - V_f^{1/3}} \tag{5}$$

Another model that has been applied to the current set of experimental data, is the simple model proposed by Counto [58], which assumes good quality of bonding between the filler and the matrix. The modulus of the composite is given by:

$$\frac{1}{E_c} = \frac{1 - V_f^{1/2}}{E_m} + \frac{1}{\frac{(1 - V_f^{1/2})}{V_f^{1/2}} + E_f} \tag{6}$$

Finally, the well-known Halpin-Tsai equations [59] were tested for their applicability. This model assumes unidirectional clay platelets and high degree of adhesion between the polymeric matrix and the filler particles. The equations that describe the specific model are:

$$\frac{E_c}{E_m} = \frac{1 + 2(L/t) V_f \eta}{1 - f_p \eta} \tag{7}$$

$$\eta = \frac{(E_p / E_m) - 1}{(E_p / E_m) + 2(L/t)} \tag{8}$$

where V_f is the particle volume fraction, L/t is the aspect ratio, E_p and E_m are the longitudinal stiffness for the particle and the matrix, respectively. The results from the application of the models on the experimental data can be seen in Figure 6.

From the results of the application of the above mentioned models, it can be seen that some are in good agreement with the experimental data while others are not. Initially, the Guth's equation fails to predict efficiently the experimental values at high filler volumes. Additionally, the modulus reduction factor that was introduced by Wu, is quite accurate at low filler content (up to 1 wt.%), but cannot predict the behavior of the composites at higher filler content. The theories proposed by Paul and Ishai and Cohen also fail to predict the modulus of elasticity for the composites, since they assume homogeneous stress transfer and perfect adhesion. Counto's theory predicts quite accurately the experimental values for filler concentrations up to 2.5 wt.%, indicating good bonding between the matrix and the filler particles. Finally, the Halpin-Tsai equations can be considered quite accurate for both sets of samples, since the correlation between theoretical and experimental values is high for concentrations up to 3.5 wt.%. This fact can be attributed to the high degree of adhesion and to undistributed orientation of the clay sheets.

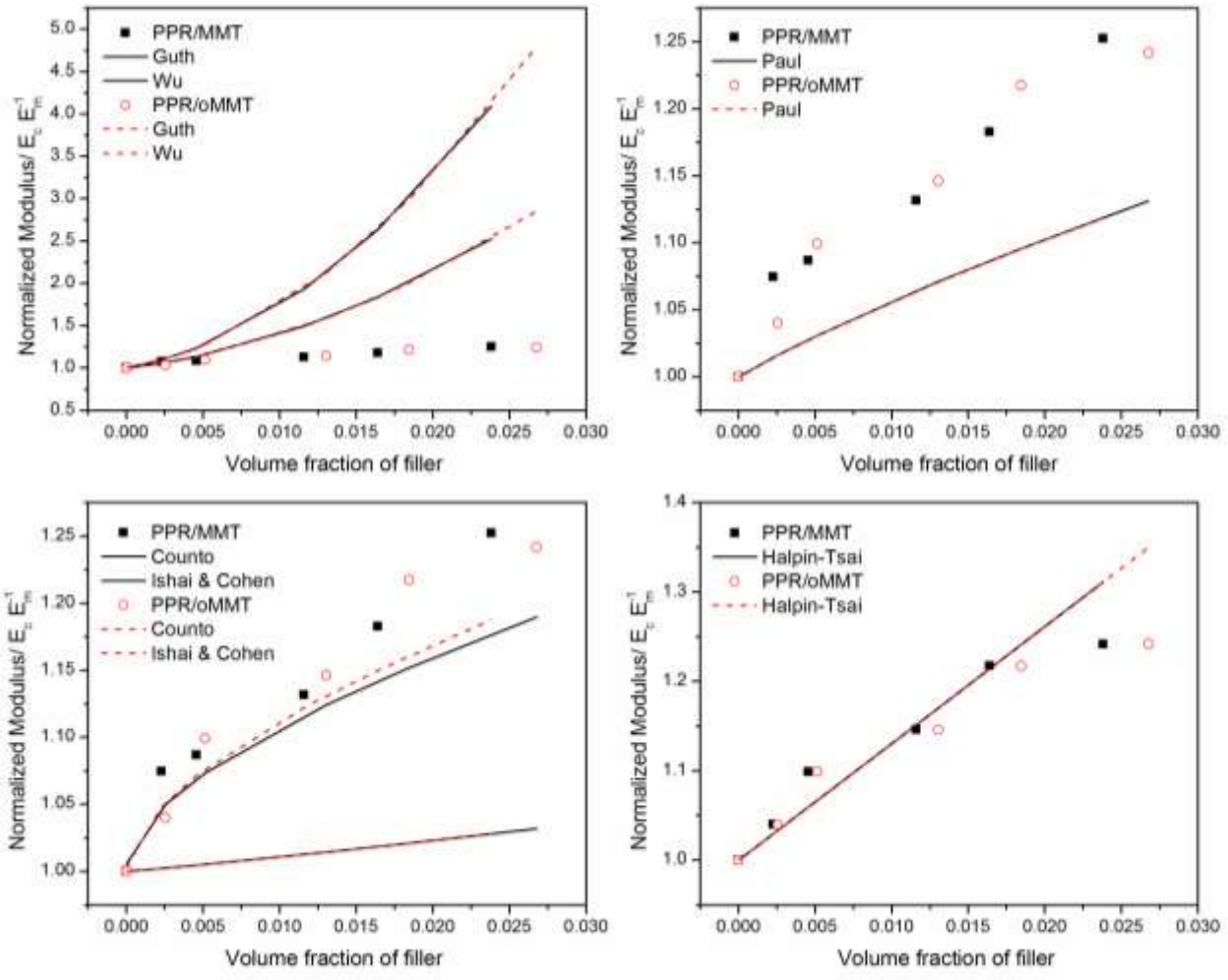

Figure 6. Modeling of the modulus of elasticity with different theories.

3.4 Thermogravimetric Analysis (TG)

The thermal degradation of PPR filled with neat and organo-modified montmorillonite was studied by means of thermogravimetric analysis (Figures 7 and 8). For the samples filled with untreated montmorillonite, the thermal stability is enhanced, both at the beginning of degradation and at the later stages. The enhancement of the thermal stability of the composites can be attributed to the confinement phenomenon of the macromolecular chains, as it was mentioned earlier. According to this theory, the clays can create locally confined areas where the

macromolecular chains of the matrix are more or less confined, thus their movement is restricted and their thermal stability is enhanced [48]. From the results presented in Table 2, it can be seen that the sample that presents the highest retardation of thermal decomposition is the one filled with 2.5 wt.% MMT, while from that point, thermal stability lowers, due to the fact that more aggregates are formed. On the other hand, the samples containing organically modified montmorillonite do not behave similar to the PPR/MMT samples, since the ammonium salts that are inserted for the improvement in the quality of dispersion of clay, are thermally not stable enough, so as to allow an enhancement of the thermal stability of the polymeric matrix throughout the decomposition process [60-62]. It should be stated that, the initial stage of decomposition (mass loss<5% - low temperature range) of the composites containing oMMT is retarded compared to the polymeric matrix, while the decomposition phenomena are more abrupt for those samples, after a mass loss percentage higher than 7-8%.

The decomposition of the reactive ammonium groups induces the fast degradation of the polymeric matrix; this was already demonstrated for several polymeric matrixes [14, 63, 64]. However, at low filler content, the thermal decomposition of the composite samples is retarded, since the amount of quarternary ammonium salts that are included is very small, therefore it does not drastically affect the decomposition. The sample filled with 0.5 wt.% oMMT is more thermally stable throughout the decomposition process, most probably due to the very small fraction of the organic modification. Generally, the low thermal stability of the alkyl-modified montmorillonite severely limits its use, since most applications demand excellent thermal stability and many polymeric matrixes exhibit higher melting points and processing temperatures than the melting point of alkyl-modified montmorillonite.

In Figures 7, 8 the mass (%) and the derivative mass (DTG) curves are presented. The thermal stability of the samples filled with untreated MMT is significantly improved for all stages of the decomposition process, while the samples containing oMMT exhibit a decreasing trend of the thermal stability at higher temperatures and faster decomposition rates at the later parts of the decomposition, with increasing filler content.

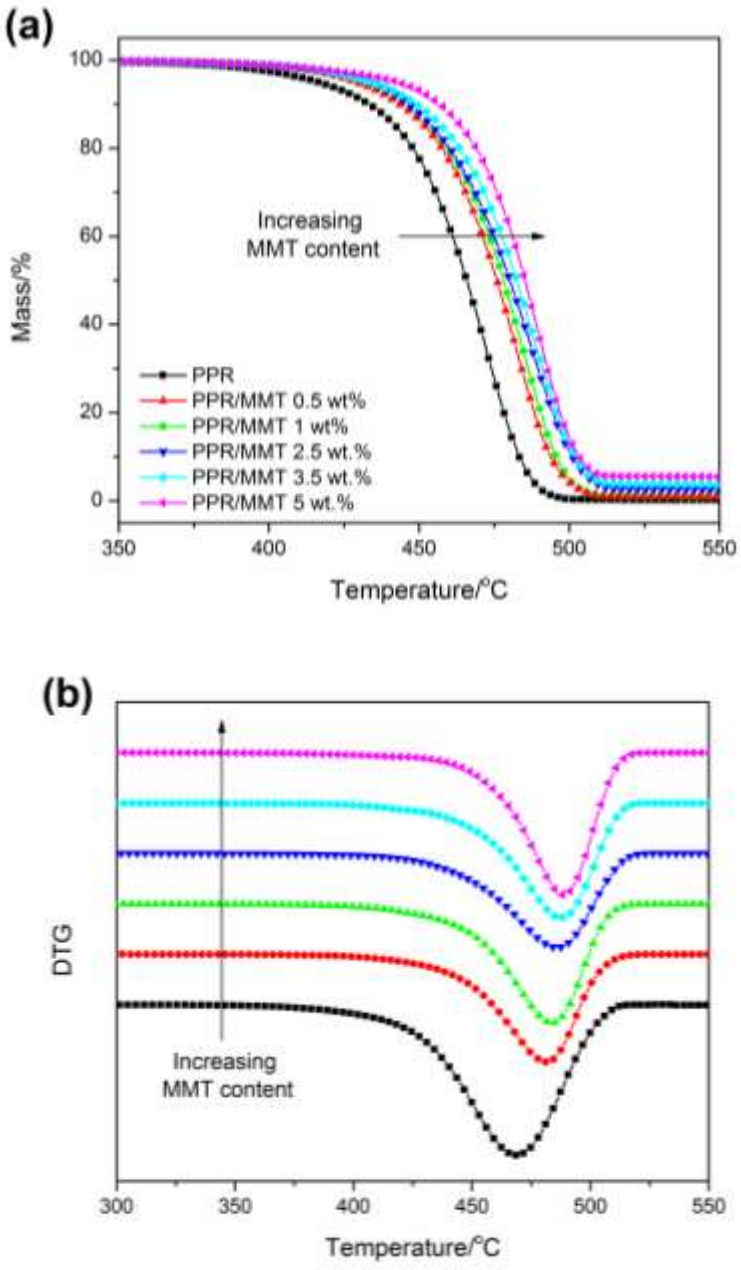

Figure 7. (a) Mass (%) versus temperature and (b) derivative mass (DTG) versus temperature at a heating rate of β=20 °C min^-1 for PPR composites with MMT.

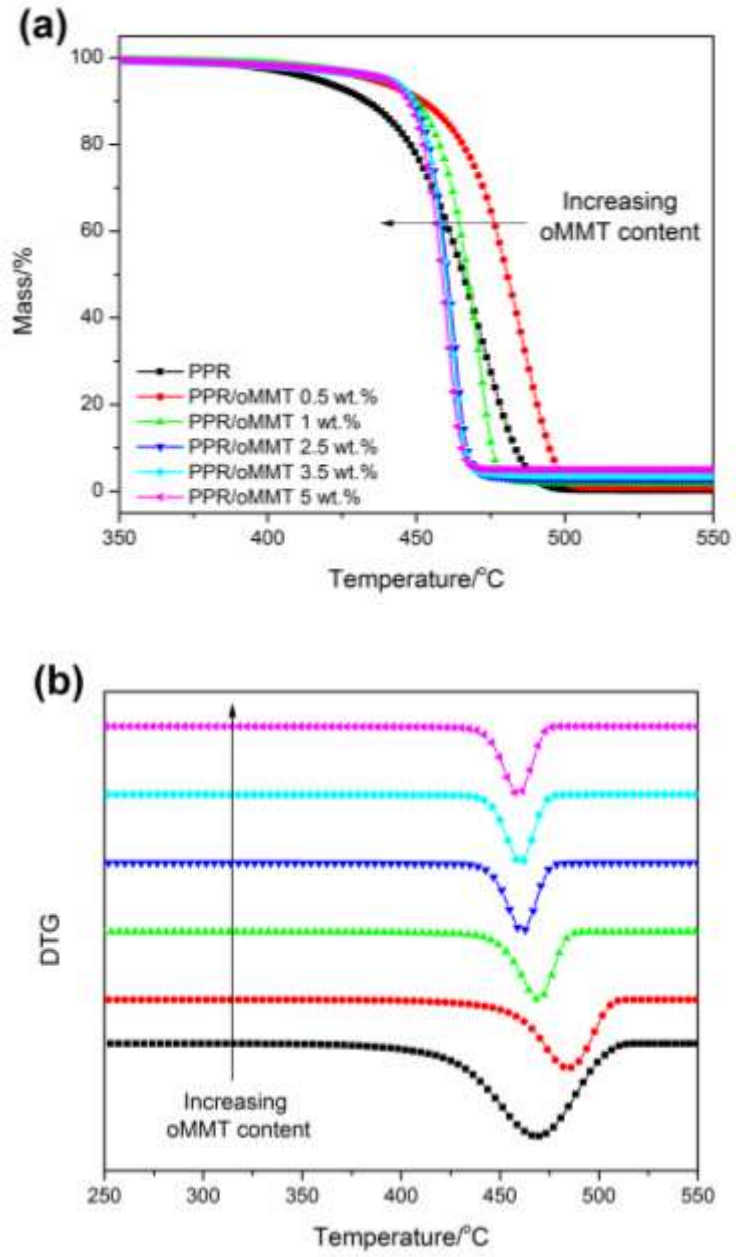

Figure 8. (a) Mass (%) versus temperature and (b) derivative mass (DTG) versus temperature at a heating rate of β=20 °C min^-1 for PPR composites with oMMT.

Table 2. Temperatures at 1% of mass loss for all samples.

MMT Content/ wt.%	$T_{1\%}$/°C	oMMT Content/ wt.%	$T_{1\%}$ /°C
0	375	0	375
0.5	395	0.5	388
1	394	1	385
2.5	396	2.5	383
3.5	394	3.5	380
5	391	5	379

3.4.1 Thermal Degradation Kinetics Study

The calculation of the kinetic parameters (E_α, α) and the conversion function $f(\alpha)$ was once again performed for both sets of samples. Thus, the experimental procedure was performed for the samples filled with 1 and 5 wt.% of neat and modified montmorillonite under multiple heating rates of 5, 10, 15 and 20°C min^-1 (Figure 9).

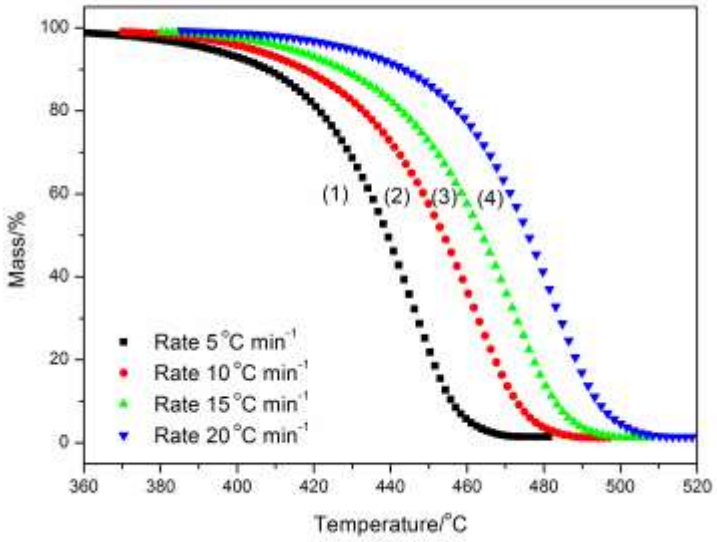

Figure 9. Mass loss (%) curves of the PPR/MMT 1 wt.% sample, under multiple heating rates: rates (1): β=5 °C min^-1, (2): β=10°C min^-1, (3): β =15 °C min^-1, (4): β=20^{o}C min^-1

3.4.1.1 Determination of the activation energy using isoconversional methods

Isoconversional methods are considered reliable for the estimation of the dependence of activation energy E_α on the degree of conversion α, since they are straightforward and abstain from the errors which are associated with the model-fitting procedures [65, 66]. It is known that, in this case, the integral isoconversional methods are mathematically incorrect [67] so that the differential method of Friedman has been employed for the series of experiments performed at different temperature programs. The dependence of the two parameters was studied for both sets of samples in order to export some useful conclusions regarding the route that should be followed during the model-fitting procedure. The fact that those methods do not employ any assumption regarding the reaction mechanism has as a direct consequence the calculation of E_α and α only, leaving out the pre-exponential factor or any kinetic exponent. The differential method of Friedman has been employed for the series of experiments performed at different temperature programs.

Friedman proposed the use of the logarithm of the conversion rate as a function of the reciprocal temperature, thus the equation which represents his theory is [68]:

$$\ln\left(\frac{d\alpha}{dt}\right)_{\alpha,i} = \ln\left(\beta\frac{d\alpha}{dT}\right)_{\alpha,i} = \ln[A_\alpha f(X)] - \frac{E_\alpha}{RT_{\alpha,i}} \quad (9)$$

The subscript i denotes different heating rates, β is the heating rate, R the universal gas constant and T is the temperature at which the extent of conversion is reached under a temperature program. The activation energy values can be calculated from the plots of ln[β(da/dt)] versus $1/T_\alpha$ obtained from the thermogravimetric data from different heating rates.

The results from the application of Friedman's method can be seen in Figure 10.

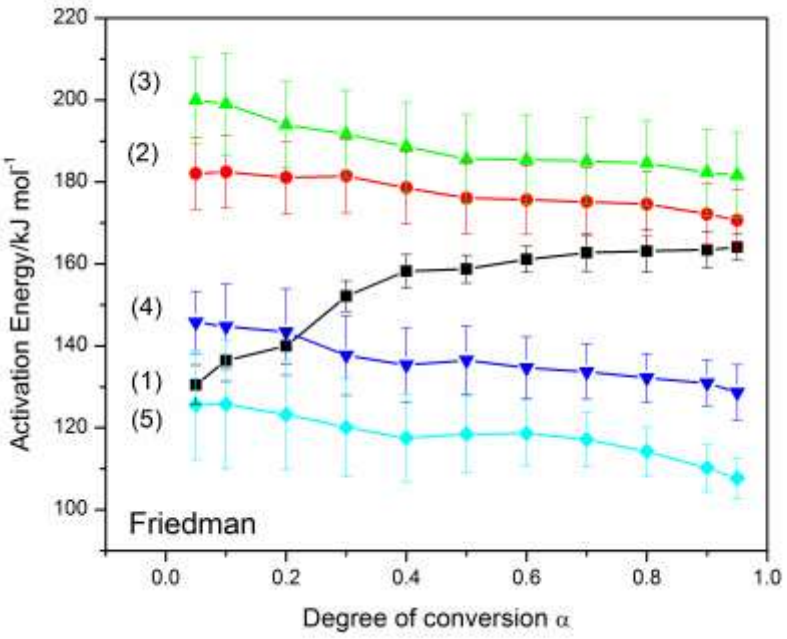

Figure 10. Dependence of the activation energy E_α on the degree of conversion α, according to Friedman's method for (1) PPR, (2) PPR/MMT 1 wt.%, (3) PPR/MMT 5 wt.%, (4) PPR/oMMT 1 wt.%, (5) PPR/oMMT 5 wt.%

We initially conclude from Figure 10 that the samples filled with neat MMT present higher values of activation energy compared to the polymeric matrix, while the samples containing organically-modified MMT present for the most part lower values of activation energy than the other samples. It is interesting that the sample filled with 1 wt.% oMMT presents higher activation energy values than the polymeric matrix for low degrees of conversion (α<0.3) since at the early stages of degradation, the sample presents slightly higher thermal stability as a result of the relatively low amount of ammonium salts contained in the filler. The relatively stable behavior of the curves for all degrees of conversion for some samples, may indicate that one decomposition mechanism may be able to describe the decomposition process during the model fitting procedure; however the presence of two mechanisms should also be examined, since the

degradation of process of polymer composites involves complex reactions [67]. The use of two mechanisms is considered quite usual for this type of analysis.

3.4.1.2 Determination of the activation energy using model-fitting methods

The dependence of E_α on conversion shown in Figure 10 indicates that the degradation mechanism is complex [67]. Hence, the multivariate non-linear regression study for the determination of the most possible kinetic model or combination of kinetic models for the decomposition of the samples filled with MMT and oMMT was performed for both sets of samples. The specific method does not assume knowledge of the activation energy and the conversion function in advance. The quality of the fitting was determined according to the regression coefficient and various combinations of 16 theoretical models were tested for their applicability on the current set of data. The first part of the model-fitting process involves the calculation of the kinetic triplet (E_α $f(\alpha)$, A), after applying a single-step model for the description of thermal degradation of the composite samples. The single-step theoretical model that better fits the thermogravimetric curves for all samples, is the n-order model with autocatalysis (*Cn*). The results from the application of this model will be shown for brevity reasons only for the samples filled with 1 wt.% MMT and 5 wt.% oMMT (Figure 11).

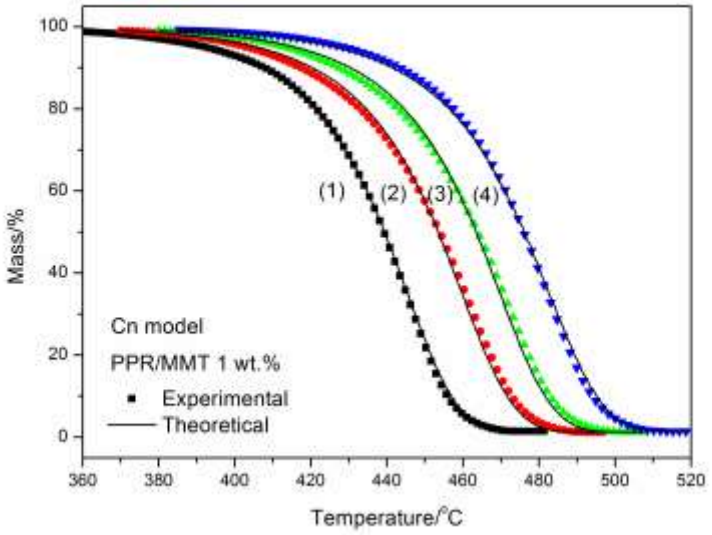

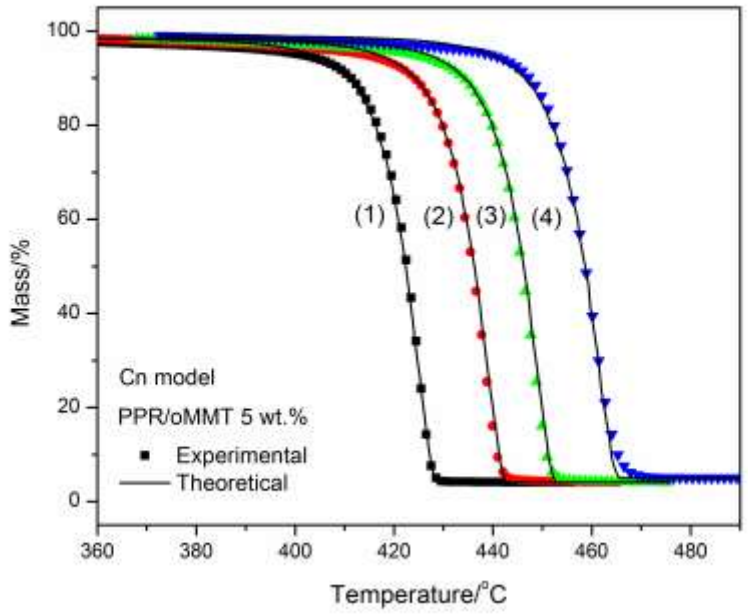

Figure 11. Mass loss experimental data and fitting curves for different heating rates (1): β=5 °C min^-1, (2): β=10°C min^-1, (3): β=15°C min^-1, (4): β=20°C min^-1 and *Cn* reaction mechanism of PPR/MMT 1 wt.% and PPR/oMMT 5 wt.% composite samples.

As it can be seen from Figure 11, the quality of fitting can be considered quite satisfactory for both samples, and the correlation coefficient is in the vincinity of 0.996-0.997. Some small diversions in the beginning and end of the decomposition process can be considered negligible. However, the presence of two or more consecutive or parallel mechanisms should be examined in terms of a minor improvement of the correlation quality and the accuracy of the activation energy values. Thus, several models and combinations have been tested for both sets of composite samples and the combination which gives the most accurate fitting, improving even more the quality of fitting than the single-step model, is the two-step consecutive *Cn-Fn* model, where *Fn* is an n-th order model. The results from the fitting with the *Cn-Fn* consecutive model are presented in Figure 12 and Table 3 for all composite samples under examination.

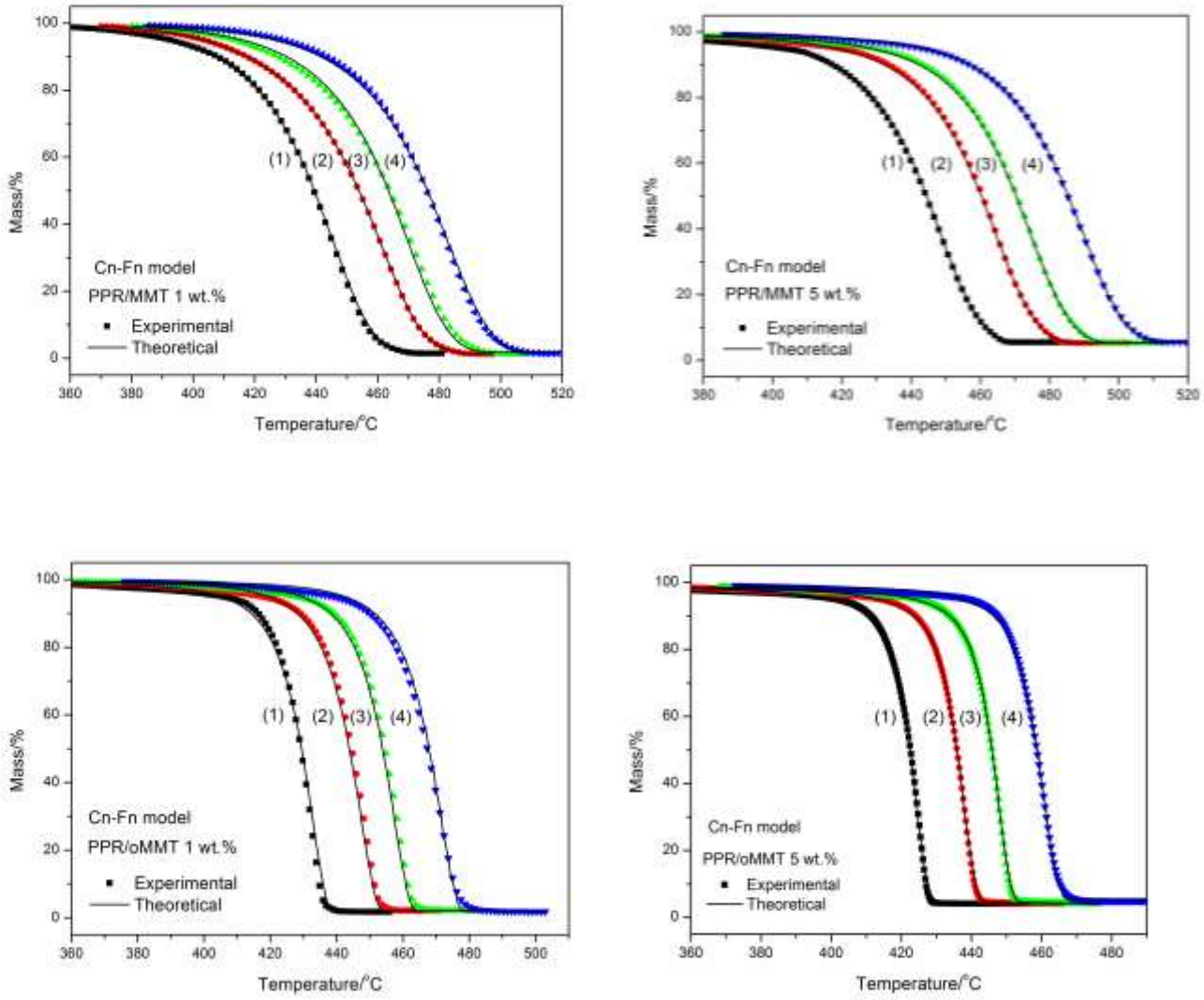

Figure 12. Mass loss experimental data and fitting curves from different heating rates for the composite samples under study. Heating rates (1): β=5 °C min^-1, (2): β =10°C min^-1, (3): β =15 °C min^-1, (4): β =20°C min^-1. The fitting model that was used in both cases was the n-order model (*Cn*) and the consecutive n-th order model with autocatalysis (*Fn*).

Table 3. Calculated values of activation energy (E_α), pre-exponential factor (log$A$), reaction order (n), branching rate constant (K_{cat}) and correlation coefficient (R^2) for PPR and composite samples

1st Step						
Sample	**Theoretical Model**	***E*/ kJ mol^-1**	**log*A***	***n***	**logK_{cat}**	***R^2***
PPR	*Fn*	124	9	0.5	-	0.9998
PPR/MMT 1 wt.%	*Cn*	145	8.8	0.8	0.6	0.9999
PPR/MMT 5 wt.%	*Cn*	159	6.9	0.6	1.3	0.9999
PPR/oMMT 1 wt.%	*Cn*	135	6.6	0.6	1.1	0.9999
PPR/oMMT 5 wt.%	*Cn*	131	5.5	0.5	2.4	0.9998
2nd Step						
Sample	**Theoretical Model**	***E*/ kJ mol^-1**	**log*A***	***n***	**logK_{cat}**	***R^2***
PPR	*Cn*	153	11	0.7	0.5	0.9998
PPR/MMT 1 wt.%	*Fn*	160	8.3	1	-	0.9999
PPR/MMT 5 wt.%	*Fn*	183	7	1.1	-	0.9999
PPR/oMMT 1 wt.%	*Fn*	129	3.3	0.5	-	0.9999
PPR/oMMT 5 wt.%	*Fn*	118	5.5		-	0.9998

From the results presented in Table 3, it can be seen that the theoretical models that describe the decomposition mechanism of the polymeric matrix (*Fn*→*Cn*), are different in the case of the composite samples (*Cn*→*Fn*). This is an interesting finding, which indicates that the presence of neat and organically modified clays affects the degradation route of the material and alters the decomposition mechanism. Additionally, the small drop in the activation energy values from the first to the second step, for the samples with the organically modified MMT, can be associated with the accelerated decomposition due to the presence of the ammonium salts.

4. Conclusions

The effect of neat and organically-modified clay on the structure-property relationships and thermal degradation kinetics of a β-nucleated polypropylene matrix, has been investigated. HAADF-STEM observations revealed that oMMT was dispersed better in the polymeric matrix than neat MMT. XRD experiments showed that the presence of clay inhibits the formation of β-crystals for the quenched samples, since the peak of the β-crystals that appears on the diffractogram of the matrix, disappears with the insertion of the fillers. The mechanical properties of the samples reveal some small differences between the two composites, due to the better dispersion of oMMT inside the PPR matrix, as confirmed from HAADF-STEM measurements. Additionally, several micromechanical models were tested for their validity based on the experimental results and useful conclusions were exported about the mechanical behavior of the samples. The confinement effect of the clays on the macromolecular chains of the matrix, leads to an increase of the thermal stability of the samples containing the unmodified clay, while the presence of quarternary ammonium salts drastically accelerates the decomposition of the PPR/oMMT samples, since their presence initiates thermal degradation at significantly lower temperatures. Finally the thermal degradation kinetics study revealed that the presence of clays alters the decomposition mechanism of the polymeric matrix.

Acknowledgement

This research has been co-financed by the European Union (European Social Fund – ESF) and Greek national funds through the Operational Program "Education and Lifelong Learning" of the National Strategic Reference Framework (NSRF) – Research Funding Program: Heracleitus II. Investing in knowledge society through the European Social Fund.
The authors appreciate financial support from the European Union under the Seventh Framework Program (Integrated Infrastructure Initiative No. 262348 European Soft Matter Infrastructure, ESMI).

References

1. Usuki A, Kojima Y, Kawasumi M, Okada A, Fukushima Y, Kurauchi T et al. Synthesis of nylon 6-clay hybrid. Journal of Materials Research. 1993;8(5):1179-84.
2. Kojima Y, Usuki A, Kawasumi M, Okada A, Fukushima Y, Kurauchi T et al. Mechanical properties of nylon 6-clay hybrid. Journal of Materials Research. 1993;8(5):1185-9.
3. Giannelis EP. Polymer layered silicate nanocomposites. Advanced materials. 1996;8(1):29-35.
4. LeBaron PC, Wang Z, Pinnavaia TJ. Polymer-layered silicate nanocomposites: an overview. Applied clay science. 1999;15(1):11-29.
5. Sinha Ray S, Okamoto M. Polymer/layered silicate nanocomposites: a review from preparation to processing. Progress in polymer science. 2003;28(11):1539-641.
6. Krishnamoorti R, Vaia RA, Giannelis EP. Structure and dynamics of polymer-layered silicate nanocomposites. Chemistry of Materials. 1996;8(8):1728-34.
7. Kornmann X, Lindberg H, Berglund LA. Synthesis of epoxy–clay nanocomposites: influence of the nature of the clay on structure. Polymer. 2001;42(4):1303-10.
8. Liu X, Wu Q, Berglund LA, Fan J, Qi Z. Polyamide 6-clay nanocomposites/polypropylene-grafted-maleic anhydride alloys. Polymer. 2001;42(19):8235-9.
9. Shelley J, Mather P, DeVries K. Reinforcement and environmental degradation of nylon-6/clay nanocomposites. Polymer. 2001;42(13):5849-58.
10. Brune DA, Bicerano J. Micromechanics of nanocomposites: comparison of tensile and compressive elastic moduli, and prediction of effects of incomplete exfoliation and imperfect alignment on modulus. Polymer. 2002;43(2):369-87. doi:http://dx.doi.org/10.1016/S0032-3861(01)00543-2.
11. Masenelli-Varlot K, Reynaud E, Vigier G, Varlet J. Mechanical properties of clay-reinforced polyamide. Journal of Polymer Science Part B: Polymer Physics. 2002;40(3):272-83.
12. Sheng N, Boyce MC, Parks DM, Rutledge G, Abes J, Cohen R. Multiscale micromechanical modeling of polymer/clay nanocomposites and the effective clay particle. Polymer. 2004;45(2):487-506.
13. Antoniadis G, Paraskevopoulos KM, Vassiliou AA, Papageorgiou GZ, Bikiaris D, Chrissafis K. Nonisothermal melt-crystallization kinetics for in situ prepared poly(ethylene terephthalate)/monmorilonite (PET/OMMT). Thermochimica Acta. 2011;521(1–2):161-9. doi:http://dx.doi.org/10.1016/j.tca.2011.04.019.
14. Vassiliou AA, Chrissafis K, Bikiaris DN. In situ prepared PET nanocomposites: Effect of organically modified montmorillonite and fumed silica nanoparticles on PET physical properties and thermal degradation kinetics. Thermochimica Acta. 2010;500(1–2):21-9. doi:http://dx.doi.org/10.1016/j.tca.2009.12.005.
15. Maria HJ, Lyczko N, Nzihou A, Joseph K, Mathew C, Thomas S. Stress relaxation behavior of organically modified montmorillonite filled natural rubber/nitrile rubber nanocomposites. Applied Clay Science. 2014;87(0):120-8. doi:http://dx.doi.org/10.1016/j.clay.2013.10.019.
16. Mejía A, García N, Guzmán J, Tiemblo P. Surface modification of sepiolite nanofibers with PEG based compounds to prepare polymer electrolytes. Applied Clay Science. 2014;95(0):265-74. doi:http://dx.doi.org/10.1016/j.clay.2014.04.023.
17. Yin H, Ma L, Gan M, Li Z, Shen X, Xie S et al. Preparation and properties of poly(2,3-dimethylaniline)/organic–kaolinite nanocomposites via in situ intercalative polymerization.

Composites Science and Technology. 2014;94(0):139-46. doi:http://dx.doi.org/10.1016/j.compscitech.2014.01.021.
18. Liu P, Zhu L, Guo J, Wang A, Zhao Y, Wang Z. Palygorskite/polystyrene nanocomposites via facile in-situ bulk polymerization: Gelation and thermal properties. Applied Clay Science. (0). doi:http://dx.doi.org/10.1016/j.clay.2014.06.023.
19. Greesh N, Sanderson R, Hartmann PC. Functionalization of montmorillonite by end-chain mono-cationic polystyrene and end-chain mono-cationic poly(styrene-b-2-hydroxethyl acrylate). Applied Clay Science. 2014;93–94(0):38-47. doi:http://dx.doi.org/10.1016/j.clay.2013.12.028.
20. Neppalli R, Causin V, Marega C, Modesti M, Adhikari R, Scholtyssek S et al. The effect of different clays on the structure, morphology and degradation behavior of poly(lactic acid). Applied Clay Science. 2014;87(0):278-84. doi:http://dx.doi.org/10.1016/j.clay.2013.11.029.
21. Varga J. β-modification of isotactic polypropylene: Preparation, structure, processing, properties, and application. Journal of Macromolecular Science - Physics. 2002;41 B(4-6):1121-71.
22. Menyhárd A, Varga J, Molnár G. Comparison of different -nucleators for isotactic polypropylene, characterisation by DSC and temperature-modulated DSC (TMDSC) measurements. Journal of Thermal Analysis and Calorimetry. 2006;83(3):625-30.
23. Jones AT, Aizlewood JM, Beckett DR. Crystalline forms of isotactic polypropylene. Die Makromolekulare Chemie. 1964;75(1):134-58. doi:10.1002/macp.1964.020750113.
24. Varga J, Mudra I, Ehrenstein GW. Crystallization and melting of β-nucleated isotactic polypropylene. Journal of Thermal Analysis and Calorimetry. 1999;56(3):1047-57.
25. Menyhárd A, Dora G, Horváth Z, Faludi G, Varga J. Kinetics of competitive crystallization of β- and α- modifications in β-nucleated iPP studied by isothermal stepwise crystallization technique. Journal of Thermal Analysis and Calorimetry. 2012;108(2):613-20.
26. Chen HB, Karger-Kocsis J, Wu JS, Varga J. Fracture toughness of α- and β-phase polypropylene homopolymers and random- and block-copolymers. Polymer. 2002;43(24):6505-14. doi:http://dx.doi.org/10.1016/S0032-3861(02)00590-6.
27. Bárány T, Izer A, Karger-Kocsis J. Impact resistance of all-polypropylene composites composed of alpha and beta modifications. Polymer Testing. 2009;28(2):176-82.
28. Papageorgiou DG, Bikiaris DN, Chrissafis K. Effect of crystalline structure of polypropylene random copolymers on mechanical properties and thermal degradation kinetics. Thermochimica Acta. 2012;543:288-94.
29. Naffakh M, Díez-Pascual AM, Marco C, Ellis G. Novel polypropylene/inorganic fullerene-like WS2 nanocomposites containing a β-nucleating agent: Mechanical, tribological and rheological properties. Materials Chemistry and Physics. 2014;144(1–2):98-106. doi:http://dx.doi.org/10.1016/j.matchemphys.2013.12.020.
30. Bao R-Y, Cao J, Liu Z-Y, Yang W, Xie B-H, Yang M-B. Towards balanced strength and toughness improvement of isotactic polypropylene nanocomposites by surface functionalized graphene oxide. Journal of Materials Chemistry A. 2014;2(9):3190-9. doi:10.1039/c3ta14554a.
31. Dai X, Zhang Z, Wang C, Ding Q, Jiang J, Mai K. A novel montmorillonite with β-nucleating surface for enhancing β-crystallization of isotactic polypropylene. Composites Part A: Applied Science and Manufacturing. 2013;49:1-8. doi:10.1016/j.compositesa.2013.01.016.
32. Zhang Z, Wang C, Meng Y, Mai K. Synergistic effects of toughening of nano-CaCO3 and toughness of β-polypropylene. Composites Part A: Applied Science and Manufacturing. 2012;43(1):189-97. doi:http://dx.doi.org/10.1016/j.compositesa.2011.10.008.

33. Naffakh M, Marco C, Ellis G. Novel polypropylene/inorganic fullerene-like WS2 nanocomposites containing a β-nucleating agent: isothermal crystallization and melting behavior. The Journal of Physical Chemistry B. 2012;116(6):1788-95.
34. Dou Q, Meng M-R, Li L. Effect of pimelic acid treatment on the crystallization, morphology, and mechanical properties of isotactic polypropylene/mica composites. Polymer Composites. 2010;31(9):1572-84. doi:10.1002/pc.20945.
35. Duan J, Dou Q. Investigation on β-polypropylene/PP-g-MAH/surface treated talc composites. Journal of Applied Polymer Science. 2013;130(1):206-21. doi:10.1002/app.39178.
36. Duan J, Dou Q. Investigation on β-polypropylene/PP-g-MAH/ surface-treated calcium carbonate composites. Polymer Composites. 2012;33(12):2245-61. doi:10.1002/pc.22370.
37. Xie W, Gao Z, Pan WP, Hunter D, Singh A, Vaia R. Thermal degradation chemistry of alkyl quaternary ammonium Montmorillonite. Chemistry of Materials. 2001;13(9):2979-90.
38. Bhat G, Hegde RR, Kamath M, Deshpande B. Nanoclay Reinforced Fibers and Nonwovens. Journal of Engineered Fabrics & Fibers (JEFF). 2008;3(3).
39. Li X, Hu K, Ji M, Huang Y, Zhou G. Calcium dicarboxylates nucleation of β-polypropylene. Journal of applied polymer science. 2002;86(3):633-8.
40. Vyazovkin S, Burnham AK, Criado JM, Pérez-Maqueda LA, Popescu C, Sbirrazzuoli N. ICTAC Kinetics Committee recommendations for performing kinetic computations on thermal analysis data. Thermochimica Acta. 2011;520(1):1-19.
41. Vyazovkin S, Chrissafis K, Di Lorenzo ML, Koga N, Pijolat M, Roduit B et al. ICTAC Kinetics Committee recommendations for collecting experimental thermal analysis data for kinetic computations. Thermochimica Acta. 2014;590(0):1-23. doi:http://dx.doi.org/10.1016/j.tca.2014.05.036.
42. Chiu FC, Lai SM, Chen JW, Chu PH. Combined effects of clay modifications and compatibilizers on the formation and physical properties of melt-mixed polypropylene/clay nanocomposites. Journal of Polymer Science Part B: Polymer Physics. 2004;42(22):4139-50.
43. Liu X, Wu Q. PP/clay nanocomposites prepared by grafting-melt intercalation. Polymer. 2001;42(25):10013-9.
44. Tang Y, Hu Y, Zhang R, Gui Z, Wang Z, Chen Z et al. Investigation on polypropylene and polyamide-6 alloys/montmorillonite nanocomposites. Polymer. 2004;45(15):5317-26.
45. Mollova A, Androsch R, Mileva D, Gahleitner M, Funari SS. Crystallization of isotactic polypropylene containing beta-phase nucleating agent at rapid cooling. European Polymer Journal. 2013;49(5):1057-65. doi:10.1016/j.eurpolymj.2013.01.015.
46. Zheng W, Lu X, Ling Toh C, Hua Zheng T, He C. Effects of clay on polymorphism of polypropylene in polypropylene/clay nanocomposites. Journal of Polymer Science Part B: Polymer Physics. 2004;42(10):1810-6.
47. Zhu S, Chen J, Zuo Y, Li H, Cao Y. Montmorillonite/polypropylene nanocomposites: Mechanical properties, crystallization and rheological behaviors. Applied Clay Science. 2011;52(1):171-8.
48. Chen K, Wilkie CA, Vyazovkin S. Nanoconfinement revealed in degradation and relaxation studies of two structurally different polystyrene-clay systems. Journal of Physical Chemistry B. 2007;111(44):12685-92.
49. Papageorgiou DG, Tzounis L, Papageorgiou GZ, Bikiaris DN, Chrissafis K. β-nucleated propylene–ethylene random copolymer filled with multi-walled carbon nanotubes: Mechanical, thermal and rheological properties. Polymer. 2014;55(16):3758-69.

50. Papageorgiou DG, Vourlias G, Bikiaris DN, Chrissafis K. Synergistic Effect of Functionalized Silica Nanoparticles and a β-Nucleating Agent for the Improvement of the Mechanical Properties of a Propylene/Ethylene Random Copolymer. Macromolecular Materials and Engineering. 2014;299(6):707-21. doi:10.1002/mame.201300320.
51. Chen H, Karger-Kocsis J, Wu J, Varga J. Fracture toughness of α-and β-phase polypropylene homopolymers and random-and block-copolymers. Polymer. 2002;43(24):6505-14.
52. Guth E. Theory of filler reinforcement. Journal of applied physics. 2004;16(1):20-5.
53. Rooj S, Das A, Stöckelhuber KW, Wang D-Y, Galiatsatos V, Heinrich G. Understanding the reinforcing behavior of expanded clay particles in natural rubber compounds. Soft Matter. 2013;9(14):3798-808.
54. Wu Y-P, Jia Q-X, Yu D-S, Zhang L-Q. Modeling Young's modulus of rubber–clay nanocomposites using composite theories. Polymer Testing. 2004;23(8):903-9.
55. Ishai O, Cohen LJ. Elastic properties of filled and porous epoxy composites. International Journal of Mechanical Sciences. 1967;9(8):539-46.
56. Paul B. Trans Metall Soc AIME. 1960:36.
57. Fu S-Y, Feng X-Q, Lauke B, Mai Y-W. Effects of particle size, particle/matrix interface adhesion and particle loading on mechanical properties of particulate–polymer composites. Composites Part B: Engineering. 2008;39(6):933-61.
58. Counto UJ. The effect of the elastic modulus of the aggregate on the elastic modulus, creep and creep recovery of concrete. Magazine of Concrete Research. 1964;16(48):129-38.
59. Affdl J, Kardos J. The Halpin-Tsai equations: a review. Polymer Engineering & Science. 1976;16(5):344-52.
60. Xie W, Gao Z, Pan W-P, Hunter D, Singh A, Vaia R. Thermal Degradation Chemistry of Alkyl Quaternary Ammonium Montmorillonite. Chemistry of Materials. 2001;13(9):2979-90. doi:10.1021/cm010305s.
61. Chrissafis K, Bikiaris D. Can nanoparticles really enhance thermal stability of polymers? Part I: an overview on thermal decomposition of addition polymers. Thermochimica Acta. 2011;523(1):1-24.
62. Bikiaris D. Can nanoparticles really enhance thermal stability of polymers? Part II: An overview on thermal decomposition of polycondensation polymers. Thermochimica Acta. 2011;523(1-2):25-45.
63. Chen X-S, Yu Z-Z, Liu W, Zhang S. Synergistic effect of decabromodiphenyl ethane and montmorillonite on flame retardancy of polypropylene. Polymer Degradation and Stability. 2009;94(9):1520-5. doi:http://dx.doi.org/10.1016/j.polymdegradstab.2009.04.031.
64. Yu Z-Z, Yang M, Zhang Q, Zhao C, Mai Y-W. Dispersion and distribution of organically modified montmorillonite in nylon-66 matrix. Journal of Polymer Science Part B: Polymer Physics. 2003;41(11):1234-43. doi:10.1002/polb.10480.
65. Papageorgiou D, Roumeli E, Chrissafis K, Lioutas C, Triantafyllidis K, Bikiaris D et al. Thermal degradation kinetics and decomposition mechanism of PBSu nanocomposites with silica-nanotubes and strontium hydroxyapatite nanorods. Physical Chemistry Chemical Physics. 2014;16(10):4830-42.
66. Sbirrazzuoli N. Determination of pre-exponential factors and of the mathematical functions f(α) or G(α) that describe the reaction mechanism in a model-free way. Thermochimica Acta. 2013;564(0):59-69. doi:http://dx.doi.org/10.1016/j.tca.2013.04.015.

67. Šimon P, Thomas P, Dubaj T, Cibulková Z, Peller A, Veverka M. The mathematical incorrectness of the integral isoconversional methods in case of variable activation energy and the consequences. Journal of Thermal Analysis and Calorimetry. 2014;115(1):853-9. doi:10.1007/s10973-013-3459-7.
68. Friedman HL. Kinetics of thermal degradation of char-forming plastics from thermogravimetry. Application to a phenolic plastic. Journal of Polymer Science Part C: Polymer Symposia. 1964;6(1):183-95. doi:10.1002/polc.5070060121.